Chapter 7

Wired/Wireless Photonic Communication Systems Using Optical Heterodyning

Alejandro García Juárez, Ignacio Enrique Zaldívar Huerta,
Antonio Baylón Fuentes, María del Rocío Gómez Colín,
Luis Arturo García Delgado, Ana Lilia Leal Cruz and Alicia Vera Marquina

Additional information is available at the end of the chapter

http://dx.doi.org/10.5772/59081

1. Introduction

Over the past few years, there has been an increasing effort in researching new design of indoor wireless communications systems, due to connectivity that show in a room or in a building. Currently, several companies of telecommunications use purely omnidirectional antennas in their wireless routers to transmit data to laptops in close vicinity [1]. The properties of microstrip patch antennas and arrays with their planar configuration exhibit an attractive option for indoor communications where the gain is considerably enhanced. On the other hand, the generation of microwave and millimetre-wave (mm-wave) signals by using photonic techniques are being used in radio-over-fiber (RoF) systems, distribution antenna systems, broadband wireless access networks, and radar systems etc. In all these applications the microwave signals are generated at a remote central station and distributed transparently to several simplified antenna stations via optical fiber [1]. The main goal of these systems is to reduce infrastructure cost and to overcome the capacity bottleneck in wireless access networks, allowing, at the same time, flexible merging with conventional optical access networks. Thus, in order to design a reliable RoF-based access network infrastructure, RoF techniques must be capable of generating the microwave signals and allow a reliable microwave signals transmission over the optical link. For broadband wireless systems and distribution antenna systems operating at microwave and millimeter-wave carriers, several photonic techniques for generating microwave signals have been proposed. Among the most common used techniques are: optical heterodyning [2], optical injection locking [3], optical frequency/phase locked loops (OFLL/OPLL) [4], microwave generation using external modulation [5]. Optical injection locking and optical phase-locked loops (OPLL) are expensive in practice. The use of

external intensity modulation generates frequency doubling or quadrupling of the driven radiofrequency (RF) sinusoid signal [6]. This method requires an external modulator which increases both loss and cost, and is more susceptible to bias drifting of the modulators, which can affect the output spectrum. The key advantage for generating microwave or millimeter-wave signals by optical means is that very high-frequency signals with very low phase noise and high purity can be generated. By using optical heterodyne technique it is very easy to tune frequencies with a spectral linewidth of a few ten MHz and over a wide range by simply tuning the wavelength of the two optical input signals; the obtained frequencies are limited only by the photodetector bandwidth [2]. Besides, the generated signals by using this technique can be generally used as both information carriers, and as a local oscillator for transmitting and receiving both analog and digital information signals by using not only RF schemes but also through an optical fiber. On the other hand, microwave photonics, which brings together radiofrequency engineering and optoelectronics, has attracted great interest in the field of telecommunications since it is an excellent alternative for the transmission of services such as high quality audio and video, e-mail, and Internet among others [7]. Furthermore, there has been an increase effort in researching new microwave photonics techniques for different interesting application that attracts interest in research is the filtering of microwave signals by using photonic techniques. The main feature of a photonic filter is that microwave signals are directly processed in the optical domain exploiting advantages inherent to photonics such as low loss, high bandwidth, immunity to electromagnetic interference, and tunability [8]. On the other hand, network architectures such as FTTx, where x can stand for home (H), building (B), neighborhood (N), or curb (C), are a communication architecture in which the final connection to the subscribers is optical fiber. Another important application of photonic telecommunications systems, which is very closely related to the FTTx systems, is the distribution of signals by integrating optical and wireless networks and passive optical networks (PONs). This particular type of scheme is referred as fiber-radio system [9]. Along with wavelength division multiplexing (WDM) technique, it would be more advantageous if RoF is integrated with a conventional PON where a base station (BS) plays the role of an optical network unit (ONU) to support both wired and wireless services. This integrated optical access system is capable not only to reduce the cost of multifunction BSs and the whole system but also meet the demands for bandwidth, mobility and connection options of users [10]. In this sense, the purpose of this chapter is to describe two an alternative optical communications systems. The first proposed system uses a couple microstrip antennas for distributing point to point analog TV with coherent demodulation based on optical heterodyne. In the proposed experimental setup, two optical waves at different wavelengths are mixed and applied to a photodetector. Then a beat signal with a frequency equivalent to the spacing of the two wavelengths is obtained at the output of the photodetector. This signal corresponds to a microwave signal located at 2.8 GHz, which it is used as a microwave carrier in the transmitter and as a local oscillator in the receiver of our optical communication system. The feasibility of this technique is to demonstrate the transmission of a TV signal located at 66-72 MHz. The second system deals with the experimental transmission of analog TV signal in a fiber-radio scheme using a microwave photonic filter (MPF). For that purpose, filtering of a microwave band-pass window located at 2.8 GHz is obtained by the interaction of an externally modulated multi-

http://dx.doi.org/10.5772/59081

mode laser diode emitting at 1.5 μm associated to the chromatic dispersion parameter of an optical fiber. Transmission of TV signal coded on the microwave band-pass window is achieved over an optical link of 20.70 km. Demodulated signal is transmitted via radiofrequency using printed antennas.

2. Optical heterodyne technique

The basic principle for generating microwave carriers is based on optical heterodyne technique, it represents a physical process called optical beating or frequency beating, where two phase-locked optical sources with angular frequencies ω_1 and ω_2 are superimposed and injected into a high frequency photodetector that permits to obtain a photocurrent at a frequency $\omega_2 - \omega_1$. To explain this in more detail, let us consider the relation between the generated electrical output signal and the two superimposed optical input waves from a more physical point of view. For simplicity, we assume that the two optical input waves are linearly polarized monochromatic plane waves in the infrared which propagate in the +z direction. Let

$$\mathrm{E}_1 = \hat{\mathrm{E}}_1 \exp\left[i\left(\omega_1 t - k_1 z + \varphi_1\right)\right]\mathrm{e}_1, \tag{1}$$

and

$$\mathrm{E}_2 = \hat{\mathrm{E}}_2 \exp\left[i\left(\omega_2 t - k_2 z + \varphi_2\right)\right]\mathrm{e}_2, \tag{2}$$

be the complex electrical field vectors of the two optical waves, with field amplitudes $\hat{\mathrm{E}}_1$ and $\hat{\mathrm{E}}_2$, angular frequencies ω_1 and ω_2 and wave numbers k_1 and k_1 . The phase of each optical input wave is considered by φ_1 and φ_1 and e_1 and e_2 are the unit vectors determining the orientation of the electrical field vector of the linearly polarized optical input waves. The intensities of the constituent waves are given by the magnitude of their Poynting vectors and are therefore given by [11]

$$I_1 = \frac{1}{2}\left(\frac{\varepsilon_{\mathrm{r}}\varepsilon_o}{\mu_o}\right)^{1/2}\left|E_1\right|^2. \tag{3}$$

$$I_2 = \frac{1}{2}\left(\frac{\varepsilon_{\mathrm{r}}\varepsilon_o}{\mu_o}\right)^{1/2}\left|E_2\right|^2. \tag{4}$$

If the two incident optical waves are perfect plane waves and have precisely the same polarization ($e_1 = e_2$), the resulting electrical field E_o of the optical interference signal is the sum of the two constituent input fields and hence we can write $E_o = E_1 + E_2$. Taking the squared absolute value of the optical interference signal we obtain

$$\begin{aligned}\left|E_o\right|^2 &= \left|E_1 + E_2\right|^2 = \left|E_1\right|^2 + \left|E_2\right|^2 + E_1E_2^* + E_1^*E_2 \\ &= \left|E_1\right|^2 + \left|E_2\right|^2 + 2\left|E_1\right|\left|E_2\right|\cos\left((\omega_2 - \omega_1)t - (\varphi_2 - \varphi_1)\right).\end{aligned} \tag{5}$$

From equation (5) and by using equations (3) and (4), it follows that the intensity of the interference signal I_o is given by [11]

$$I_o = I_1 + I_2 + 2\left(I_1I_2\right)^{1/2}\cos\left((\omega_2 - \omega_1)t - (\varphi_2 - \varphi_1)\right). \tag{6}$$

By launching this optical interference signal into a photodetector, a photocurrent *i* is generated which can be expressed as [11]

$$i = \frac{\eta_o q}{hf_1}P_1 + \frac{\eta_o q}{hf_2}P_2 + 2\frac{\eta_{f_c} q}{h}\left(\frac{P_1P_2}{f_1f_2}\right)^{1/2}\cos\left((\omega_2 - \omega_1)t - (\varphi_2 - \varphi_1)\right), \tag{7}$$

where q is the electron charge and P_1 and P_2 denote the optical power levels of the two constituent optical input waves. The photodetector's DC and high-frequency quantum efficiencies are represented by η_o and η_{f_c} . It is of course important to consider that the detector's quantum efficiency is not independent of the frequency. Several intrinsic and extrinsic effects such as transit time limitations or microwave losses will eventually limit the high-frequency performance of the detector and thus the detector's DC responsivity η_o is typically much larger than its high-frequency responsivity η_{f_c} . In our case, we can further simplify the photocurrent equation (Eq. (7)) by considering the fact that the two optical input waves are close in frequency ($f_1 \approx f_2$) whereas the difference frequency f_c is by far smaller ($f_c = |f_2 - f_1| << f_1, f_2$). If we further assume for simplicity that the power levels of the two optical input waves are equal ($P_{opt} \approx P_1 \approx P_2$), Eq. (7) becomes [11]

$$i = 2s_oP_{opt} + 2s_{f_c}P_{opt}\cos\left(2\pi f_ct + \Delta\varphi\right). \tag{8}$$

Where $\Delta\varphi = \varphi_2 - \varphi_1$. Here $s_o = \frac{\eta_o q}{hf}$ and $s_{f_c} = \frac{\eta_{f_c} q}{hf}$ are the photodetector's DC and high frequency responsivities given in A/W. Eq. (8) is the fundamental equation describing optical hetero-

http://dx.doi.org/10.5772/59081

dyning in a photodetector. The first term is the DC photocurrent generated by the constituent optical input waves and the second term is the desired high-frequency signal oscillating at the difference frequency f_c (down-converter) or intermediate frequency (IF) [1]. In our case it represents the microwave signal that we will use as both information carriers, and as a local oscillator for transmitting and receiving TV signals in a wireless communication system.

3. Experimental scheme for generating microwave signals

The heterodyne technique for generating microwave signals has been done using the experimental setup shown in Figure 1. In this experiment, two laser diodes emitting at different wavelengths are used. One of them is a tunable laser (New Focus, model TLB-3902) which can be tuned over the C band with a channel spacing of 25 GHz, and the other one is a fiber coupled distributed feedback (DFB) laser source (Thorlabs, model S3FC1550) with a central wavelength at 1550 nm. For the generation of the microwave signals, the outputs of both lasers are coupled to optical isolators to avoid a feedback into the lasers and consequently instabilities to the system. A pair of polarization controllers is used to minimize the angle between the polarization directions of both optical sources. Thus, the polarization of the light issued from each optical source is matched and therefore, there is not degradation of the power levels in the microwave signals generated from the photodetector. The output of each controller is launched to a 3 dB coupler to combine both optical spectrums. After that, an optical output signal is received by a fast photodetector (MITEQ model SCMR-50K6G-10-20-10) with a typical gain of 25 dB, and –3 dB bandwidth of 6 GHz, The resulting photocurrent from the photodetector corresponds to the microwave beat signal which is analyzed with an Electrical Spectrum Analyzer (ESA), (Agilent model E4407B). The other optical output resulting from optical coupler is applied to an Optical Spectrum Analyzer (OSA) (Anritsu model MS9710C), for monitoring the wavelength of the two beams.

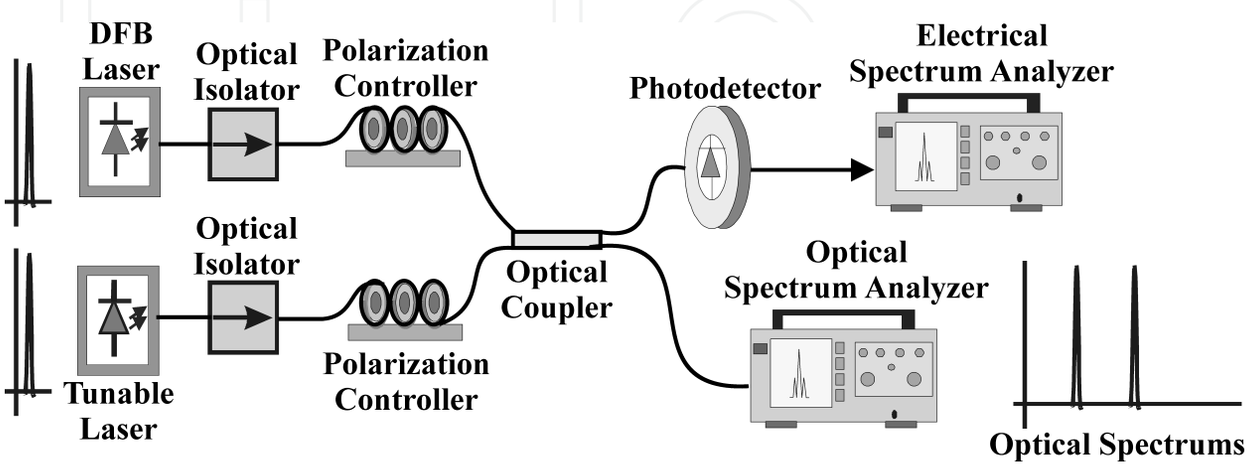

Figure 1. Experimental setup for generating microwave signals by using optical heterodyne technique.

DFB laser can be used to control not only the output power of the fiber coupled laser diode, but also the precise control of the temperature at which the laser is operating. Both controls can be used to tune the fiber coupled laser diode to an optimum operating point, providing a stable output. In this way, it is possible to observe that the wavelength of the DFB laser is shifting, by varying its temperature with a scale of 1 °C. Consequently, the beat signal frequency is continuously over the band of photodetector. On the other hand, the frequency difference from both lasers can be expressed by [1]

$$\Delta f = \frac{c}{\lambda_1} - \frac{c}{\lambda_2} = \frac{c\left(\lambda_2 - \lambda_1\right)}{\lambda_1 \lambda_2} \approx \frac{c}{\lambda^2}\left|\Delta\lambda\right|, \tag{9}$$

where λ_1 and λ_2 are the wavelengths of the two beams, respectively, and $\Delta\lambda$ is the difference between the two wavelengths. To obtain a microwave signal, in a first step, the tunable laser is biased and its optical spectrum is displayed on the OSA screen. In a second step, the DFB laser is also biased, fixing an optical power of 2.2 mW and its central wavelength is settled as near as possible to the central wavelength of the tunable laser. As can be seen from Figure 2, the value of $\Delta\lambda$ = 0.023739 nm is the wavelength difference between both lasers and it corresponds to the beat signal frequency of 2.8 GHz.

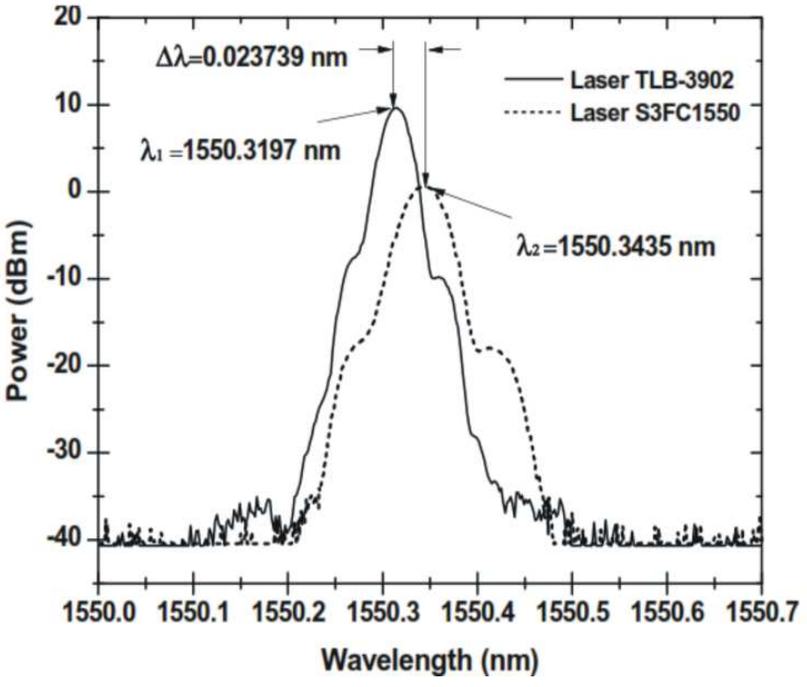

Figure 2. Optical spectrum corresponding to the mixed optical sources. The peaks located at λ_1=1550.3197 nm and λ_2=1550.3435 nm corresponds to the tunable and DFB lasers, respectively.

A precise control of the difference, between the two central wavelengths and by consequence over the frequency difference, is obtained by tuning the DFB. The wavelength variation of the

http://dx.doi.org/10.5772/59081

laser source is obtained by changing the junction temperature between 22.8 °C, 23.2 °C and 23.7 °C corresponding to the frequency range of 0 to 5.0 GHz. Figure 3 illustrates the electrical spectrums of four generated microwave signals by using optical heterodyne. These signals are located at f_1=1.0 , f_2=2.0 , f_3=2.8 and f_4=4.0 GHz respectively. It can be seen, that the microwave signals are in good agreement with theoretical value given by Eq. (9). Therefore, when one laser source is operating at a fixed wavelength and the other is being continuously tuned, the beat frequency will shift correspondingly. In particular, the frequency of the microwave drive signal is set at 2.8 GHz.

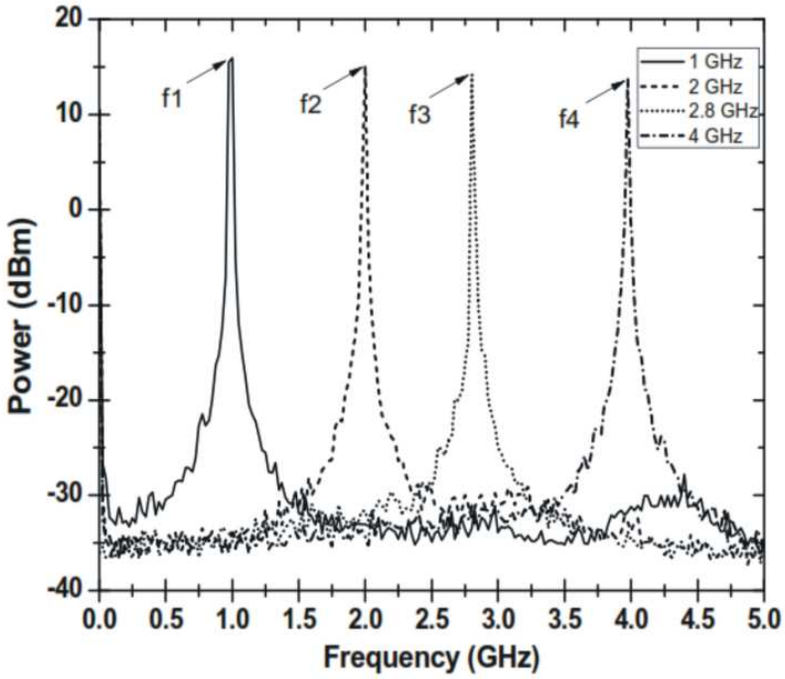

Figure 3. Spectrum for the microwave signal generated by using optical heterodyne.

4. Modulation and demodulation

Some form of modulation is always needed in an RF system to translate a baseband signal (e.g., audio, video, data) from its original frequency bandwidth to a specified RF frequency spectrum. There are many modulation techniques, for example, amplitude modulation (AM), frequency modulation (FM), amplitude shift keying (ASK), frequency shift keying (FSK), phase shift keying (PSK), biphase shift keying (BPSK), quadriphase shift keying (QPSK), 8-phase shift keying (8-PSK), 16-phase shift keying (16-PSK), minimum shift keying (MSK), and quadrature amplitude modulation (QAM). AM and FM are classified as analog modulation techniques, and the others are digital modulation techniques [12]. In this section we describe the AM modulation and demodulation due to it was used in our proposed wireless communication system.

4.1. Amplitude modulation

Analog modulation uses the baseband signal (modulating signal) to vary one of three variables: amplitude A_c , electrical frequency $(\omega_1-\omega_2)=\omega_c=2\pi f_c$; or phase $(\phi_1-\phi_2)=\Delta\phi$. According to Eq. (8), the obtained carrier signal by using optical heterodyne technique can be written by

$$p(t) = A_c \cos\left((\omega_1 - \omega_2)t + \phi_1 - \phi_2\right) = A_c \cos\left(2\pi f_c t + \Delta\phi\right). \tag{10}$$

Where $A_c=2s_{f_c}P_{opt}$. In amplitude modulation, if we assume that $s(t)$ is the information signal, and considering $A_c=1$, $\Delta\phi=0$, then a modulated signal can be written by

$$g(t) = s(t)\cos 2\pi f_c t. \tag{11}$$

Applying the modulation property of the Fourier transform to Eq. (11), we can find the density spectral of $g(t)$ is

$$G(f) = \frac{1}{2}S(f - f_c) + \frac{1}{2}S(f + f_c). \tag{12}$$

Amplitude modulation therefore translates the frequency spectrum of a signal by $\pm f_c$ hertz, but leaves the spectral shape unaltered. This type of amplitude modulation is called suppressed-carrier because the spectral density of $g(t)$ has no identifiable carrier in it, although the spectrum is centered at the frequency f_c .

4.2. Amplitude demodulation

Recovery the signal information $s(t)$ from the signal $p(t)$ requires another translation in frequency to shift the spectrum to its original position. This process is called demodulation or detection. Because the modulation property of the Fourier transform proved useful in translating spectra for modulation, we try it again for demodulation. Assuming that $g(t)=s(t)\cos 2\pi f_c t$ is the transmitted signal, we have

$$g(t)\cos 2\pi f_c t = s(t)\cos^2 2\pi f_c t = \frac{1}{2}s(t) + \frac{1}{2}\cos 4\pi f_c t. \tag{13}$$

Taking the Fourier transform of both sides of Eq. (13) and using the modulation property, we get

$$\Im\left[g(t)\cos 2\pi f_c t\right] = \frac{1}{2}S(f) + \frac{1}{4}S(f + 2f_c) + \frac{1}{4}S(f - 2f_c). \tag{14}$$

http://dx.doi.org/10.5772/59081

The mathematical process described in this section can be obtained by convolving the spectrum of the received signal $g(t)$ with that of $\cos 2\pi f_c t$ (i.e., with impulses at $\pm f_c$). A low-pass filter is required to separate out the double frequency terms from the original spectral components. Obviously we need a filter with a cut frequency $f_{cut} > 2f_m$ for proper signal recovery. In this case f_m represents the information frequency.

4.3. Effects in frequency and phase variations

When the local oscillator at the receiver, has a small frequency error Δf and a phase error $\Delta\theta$, then this signal can be written as

$$p_L(t) = \cos\left[2\pi\left(f_c + \Delta f\right)t + \Delta\theta\right]. \tag{15}$$

Assuming again that $g(t)=s(t)\cos 2\pi f_c t$ is the transmitted signal; then we have that at the receiver, the recovered signal can be written by

$$\begin{aligned} g(t)\cos\left[2\pi(f_c + \Delta f)t + \Delta\theta\right] &= s(t)\cos(2\pi f_c t)\cos\left[2\pi(f_c + \Delta f)t + \Delta\theta\right] \\ &= s(t)\left(\frac{\cos(2\pi\Delta f t + \Delta\theta)}{2} + \frac{\cos\left[2\pi(2f_c + \Delta f)t + \Delta\theta\right]}{2}\right). \end{aligned} \tag{16}$$

The second term on the right hand side of Eq. (16) is centered at $\pm 2f_c + \Delta f$ and can be filtered out by using a low pass filter. The output of this filter $s_F(t)$ will then be given by the remaining term in Eq. (16).

$$s_F(t) = \left[\frac{s(t)}{2}\left(\cos 2\pi(\Delta f)t\cos(\Delta\theta) - sen2\pi(\Delta f)tsen(\Delta\theta)\right)\right]. \tag{17}$$

As can been from equation (17), the output signal is not $\frac{s(t)}{2}$, unless both Δf and $\Delta\theta$ are zero. The effects of both frequency errors and random phase errors render this demodulation of the signal unsatisfactory. It is necessary, therefore, to have synchronization in both frequency and phase between the transmitter and the receiver when amplitude modulation is used. The synchronization of the carrier signals presents no major problem when the transmitter and the receiver are in close proximity. Recovering the original signal $s(t)$ from the modulated signal $g(t)$ using a synchronized oscillator is called coherent demodulation. In our case we take advantage of proposed optical heterodyne technique permits to obtain microwave carrier and local oscillator simultaneously in the transmitter and receiver respectively.

5. Design of a patch antenna at 2.8 GHz

The microstrip patch antenna is a popular printed resonant antenna for narrow-band microwave wireless links that require semihemispherical coverage. Due to its planar configuration and ease of integration with microstrip technology, the microstrip patch antenna has been studied heavily and is often used as an element for an array. Common microstrip antenna shapes are square, rectangular, circular, ring, equilateral triangular, and elliptical, but any continuous shape is possible [13]. Furthermore, a patch antenna is an excellent device due to its small size, low cost, and good performance [14-16]. In this chapter, a rectangular printed patch antenna is proposed. Simulation results have been obtained by using Advanced Design System (ADS) that is a computer-aided-engineering software tool. The radiating structure consists of a patch and a microstrip inset-feed line, allowing that the characteristic impedance (Zo) to be improved. Figure 4 shows the geometry and configuration of the top layer. The proposed antenna in this work was designed to operate in the band S of telecommunications (2.8 GHz). FR4 is used as a dielectric substrate exhibiting a thickness $h = 1.524mm$, and relative dielectric constant $\varepsilon_r = 4.2$. In a first step, the width (W) of the patch is computed by using [17]:

$$W = \frac{c_o}{2f_c}\sqrt{\frac{2}{\varepsilon_r + 1}}, \tag{18}$$

where c_o is the light velocity in the free space, and f_o is the operation frequency. Next, the value of the effective dielectric constant ε_{eff} is evaluated considering $W/h > 1$.

$$\varepsilon_{eff} = \frac{\varepsilon_r + 1}{2} + \frac{\varepsilon_r - 1}{2}\left(1 + 12\frac{h}{W}\right)^{-1/2} \tag{19}$$

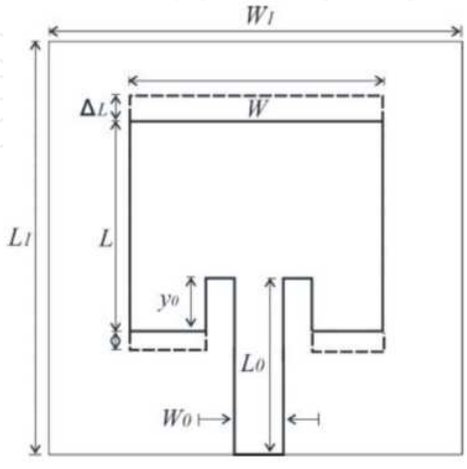

Figure 4. Layout of the patch antenna.

Border effects [17] must to be considered in the design of the antenna. For this reason, ΔL from Figure 4 can be evaluated as:

$$\frac{\Delta L}{h} = 0.412 \frac{\left(\varepsilon_{eff} + 0.3\right)\left(\frac{W}{h} + 0.264\right)}{\left(\varepsilon_{eff-0.258}\right)\left(\frac{W}{h} + 0.8\right)} \tag{20}$$

This allows that the length (L) of the patch to be evaluated as:

$$L = \frac{c_o}{2 f_o \sqrt{\varepsilon_r}} - 2\Delta L \tag{21}$$

Considering the values previously obtained, the effective dimensions (L_{eff} and W_{eff}) can be calculated, respectively as:

$$L_{eff} = L + 2\Delta L \tag{22}$$

$$W_{eff} = W + \frac{t}{\pi}\left(1 + \ln\left(\frac{2h}{t}\right)\right) \tag{23}$$

From Eq. (23), t is the conductor thickness and $W/h > 1/2\pi$ must to be considered. The ground plane dimensions are computed as:

$$\begin{aligned} L_1 &= 6h + L_{eff} \\ W_1 &= 6h + W_{eff} \end{aligned} \tag{24}$$

The best dimensions which assure a good matching between the impedances ($R_{in} = Z_o = 50\Omega$) of the antenna and generator can be calculated by the use of LineCalc tool from ADS and by the next expression:

$$R_{in}\left(y = y_o\right) = \frac{1}{2\left(G_1 \pm G_{12}\right)} \cos^2\left(\frac{\pi}{L} y_o\right) \tag{25}$$

where G_1 and G_{12} are the conductance values obtained by the cavity method. Finally, Table 1 shows a summary of the dimensions for the patch and the ground plane.

Operation Frequency (Antenna)	Dimensions (cm)						
	W_o	L_o	W	L	W_1	L_1	y_o
2.8 GHz	0.13	3.08	3.32	2.56	10	10	0.93

Table 1. Dimensions of the fabricated antenna.

Figure 5(a) shows a picture of the fabricated patch antenna where a SubMiniature version A (SMA) connector is added. Figure 5(b) illustrates simulation and experimental results corresponding to the S_{11} parameter. Electrical measurements are obtained by using a Vector Network Analyzer (VNA) (Agilent Technologies model: E8361A). It is clearly observable that experimental result is in good agreement with the simulation.

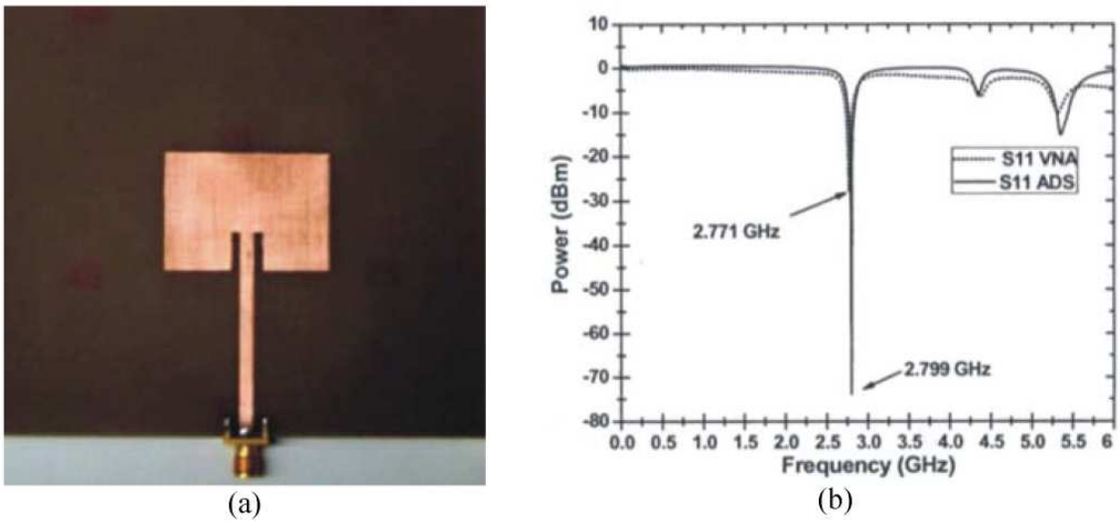

Figure 5. Fabricated antenna (a), Experimental and simulation return loss curve for the antenna (b).

6. Transmission of TV signals by using heterodyne technique

In order to show a potential application of optical heterodyne technique in the field of the wireless communications, we have proposed a coherent wired/wireless photonic communication system as shown in Figure 6. This system is not a truly wireless communication system, since an optical fiber is required to deliver both microwave carrier and local oscillator for transmitting and receiving information of TV signals as an approximation to point to point indoor wireless communications systems. From the photodetector 1 in the transmitter, a microwave signal located at 2.8 GHz is obtained and mixed with an analog TV signal located at 62.25 MHz. Then the resulting signal is amplified before being applied to our fabricated microstrip antenna. After that, the obtained modulated signal as shown in Figure 7, is transmitted through a point to point wireless link by using the microstrip antenna. Finally in the receiver, another microstrip antenna is used to receive the transmitted information, which

http://dx.doi.org/10.5772/59081

it is processed using optical heterodyne technique again to recover in this case the TV signal (66-72 MHz). From the photodetector 2 in the receiver, a local oscillator that is synchronized, in frequency as well as in phase with to that obtained from the photodetector 1, is mixed with the received signal. Then the resulting signal is filtered and the power spectral density obtained is displayed on an electrical spectrum analyzer, where it is analyzed to measure the power level of recovered information.

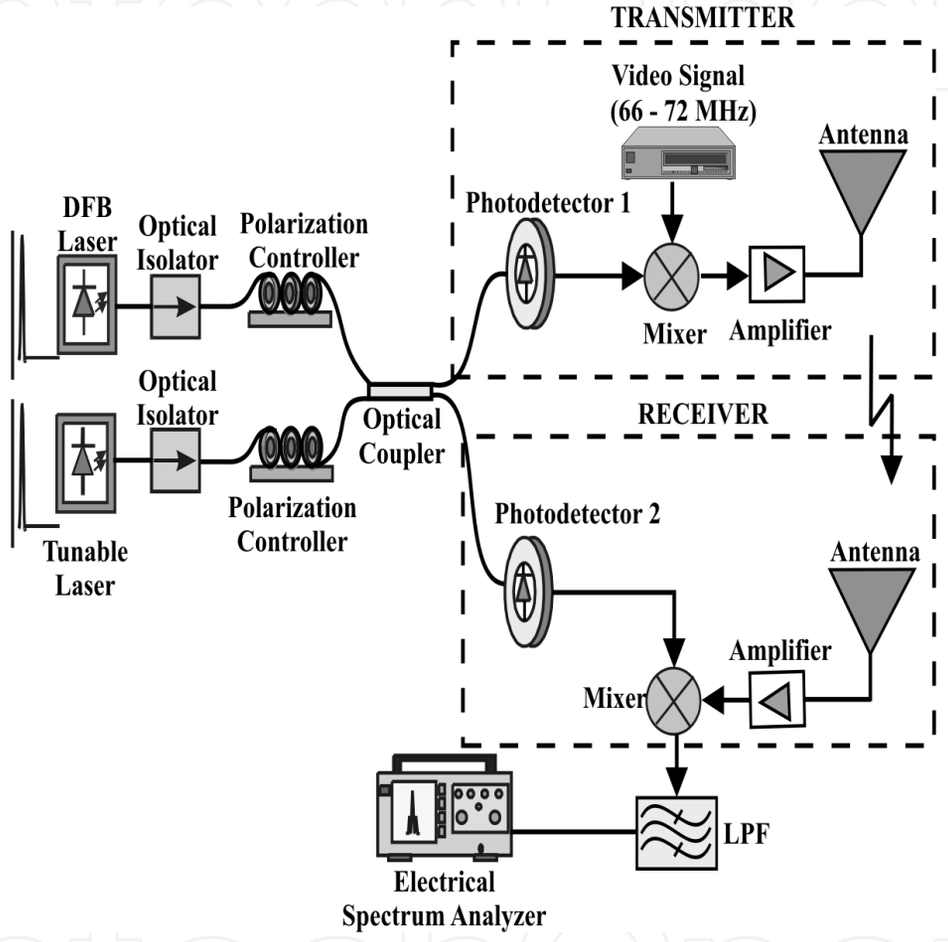

Figure 6. Wired/wireless photonic communication system for transmitting and receiving TV signals.

Figure 8 shows the frequency spectrum of an analog National Television System Committee (NTSC) TV signal at the input of the transmitter located at 67.25 MHz (before being applied to frequency mixer). In the same figure we can see the obtained analog NTSC TV signal at the output of the receiver. In order to measure the quality of the received signal, it is necessary to quantify the parameter of signal-to-noise ratio (SNR), in this case it is approximately 45 dB. The analog information is successfully transmitted from the transmitter to the receiver, and the received signal is satisfactorily reproduced on TV monitor. The differential gain and differential phase were not measured Nevertheless we demonstrated that the generated microwave signal by using optical heterodyning can be used as carrier information in a traditional communication system and we have used a TV signal of test to verify it.

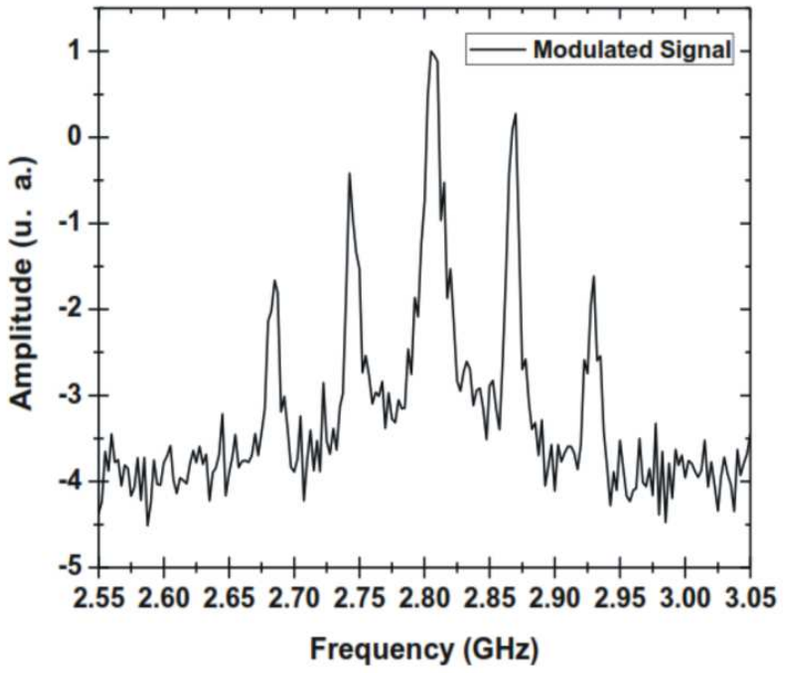

Figure 7. Electrical spectrum of the modulated signal.

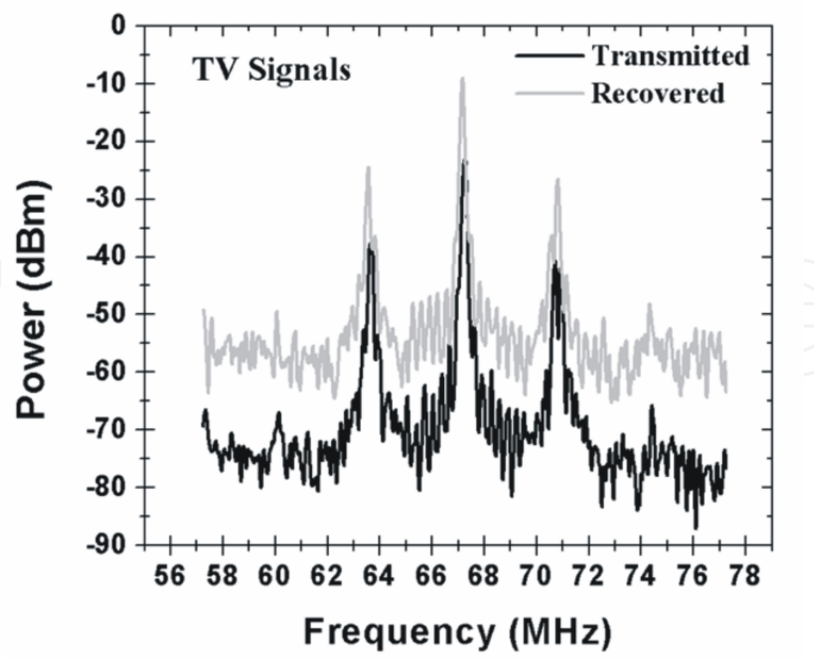

Figure 8. TV signals at 67.25 MHz, transmitted and recovered.

7. Analytical model of the microwave photonic filter

The scheme of the MPF is illustrated in Figure 9. Consider that the optical signal of a polychromatic source with spectrum $P(\omega)$, centered at an optical frequency ω_n, is launched into the input of the Mach-Zehnder intensity modulator (MZ-IM). A single spectral component of such an optical signal can be modeled by a stochastic process $e(t)=E_o(t)\exp(j\omega_n t)$, where $E_o(t)$ is the complex amplitude and ω_n is the optical angular frequency. If the intensity of such optical signal is externally modulated by an electrical signal $V_m=1+2m\cos(\omega_m t)$, where m is the modulation index and ω_m is the angular frequency of external modulation, then the optical field at the input of the optical fiber can be expressed by Eq. (26). The modulation index m is related to the electrical input signal amplitude, V_m, as: $2m=\pi(V_m/V_\pi)$, where V_π is the half wave voltage of the MZ-IM [18].

$$e_i(t)=e(t)s(t) \tag{26}$$

The optical fiber can be considered as a linear time invariant (LTI) system. If, for simplicity, the attenuation is ignored, then the transfer function of the optical link, for a given length L, is $H(j\omega)=\exp(-j\beta L)$, where β is the propagation constant. Thus, the optical field at the end of the link is given by

$$e_L(t)=e_i(t)\exp(-j\beta L) \tag{27}$$

Substituting $e(t)$ and $s(t)$ in Eq. (26), and then replacing this in Eq. (27), it becomes:

$$\begin{aligned} e_L(t)=E_o(t)\exp\left(j(\omega_m t-\beta L)\right)+E_o(t)m\exp\left(j\left[(\omega_m-\omega_n)t-\beta L\right]\right) \\ +E_o(t)m\exp\left(j\left[(\omega_m+\omega_n)t-\beta L\right]\right) \end{aligned} \tag{28}$$

In the frequency domain Eq. (28) can be expressed as:

$$\begin{aligned} E_L(\omega)=E_o(\omega-\omega_n)\exp(-j\beta L)+E_o\left(\omega-(\omega_n-\omega_m)\right)\exp(-j\beta L) \\ +E_o\left(\omega-(\omega_n+\omega_m)\right)\exp(-j\beta L) \end{aligned} \tag{29}$$

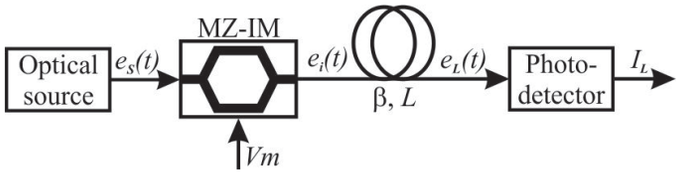

Figure 9. Scheme of the microwave photonic filter.

There are three spectral components. In the presence of chromatic dispersion, there is a propagation constant associated to each one of them, i.e. $\beta(\omega-\omega_n)$, $\beta(\omega-(\omega_n+\omega_m))$ and $\beta(\omega-(\omega_n-\omega_m))$. By denoting $W=\omega-\omega_n$, Eq. (29) then becomes:

$$\begin{aligned} E_L(\omega) = E_o(W)\exp\left(-j\beta(W)L\right) + E_o(W+\omega_m)\exp\left(-j\beta(W+\omega_m)L\right) \\ + E_o(W-\omega_m)\exp\left(-j\beta(W-\omega_m)L\right) \end{aligned} \tag{30}$$

Assuming that within the frequency range $\omega_n-\omega_m$ to $\omega_n+\omega_m$, centered at ω_n the propagation constant varies only slightly and gradually with ω , it can be approximated by the first three terms of a Taylor series expansion, and it can be shown that

$$\beta(W\pm\omega_m) = \beta(W) \pm \beta_1\omega_m + \beta_2\left[\frac{1}{2}\omega_m^2 \pm \omega_m(\omega-\omega_n)\right] \tag{31}$$

where $\beta_i=[d^i\beta(\omega)/d\omega^i]_{(\omega=\omega_n)}$.

The optical intensity, I , is obtained by integrating the power spectral density over all the frequency range, i.e.

$$I = \int_{-\infty}^{\infty} \left|E_L(\omega)\right|^2 d\omega \tag{32}$$

Considering that the MZ-IM is operating on its linear region, it is valid to note that $m^2 \approx 0$. On the other hand, if $\omega_n >> \omega_m$ then $E_o(W) \approx E_o(W+\omega_m) \approx E_o(W-\omega_m)$. Furthermore, in the frequency domain, the spectrum of the source is defined as $P(\omega)=E_o(\omega)E_o^*(\omega)$. Thus, developing the product $|E_L(\omega)|^2$ in Eq. (32) and replacing Eq. (31), it is possible to demonstrate that the intensity at the end of the optical fiber is given by:

$$I = \int_{-\infty}^{\infty} P(W)dW + 4m\cos\left(\beta_2\frac{\omega_m^2}{2}L\right)\cos(\beta_1\omega_m L)\Re\left\{\int_{-\infty}^{\infty} P(W)\exp(-j2\pi ZW)dW\right\} \tag{33}$$

where $Z=\beta_2\omega_m L/2\pi$, $W=\omega-\omega_n$ and its derivative, $dW=d\omega$. The total average intensity is $I_o=\int_{-\infty}^{\infty} P(W)dW$, and the integral $\Re\left\{\int_{-\infty}^{\infty} P(W)\exp(-j2\pi ZW)dW\right\}$ corresponds to the real part of the Fourier transform of the spectrum of the optical source. This means that the optical intensity which reaches the surface of the photodetector is proportional to:

http://dx.doi.org/10.5772/59081

$$F(W) = \Re\left\{FT\left\{P(W)\right\}\right\} \tag{34}$$

A spectrum with Gaussian shape can be modeled by an analytical expression as:

$$P(\omega) = \frac{2P_o}{\Delta\omega\sqrt{\pi}} \exp\left(-\frac{4(\omega-\omega_m)^2}{\Delta\omega^2}\right) \tag{35}$$

where ω is the angular frequency, ω is the central angular frequency, ω is the maximum power emission and $\Delta\omega$ is the full width at half maximum (FWHM) of the optical source. If the emission spectrum of the optical source has a Gaussian shape, as defined in Eq. (35), then the Eq. (34) becomes:

$$F(\omega) = \exp\left(-\left(\frac{\beta_2\omega_m L\Delta\omega}{4}\right)^2\right) \tag{36}$$

In such case the FWHM of the frequency response can be determined equating $F(\omega)=0.5$, which implies:

$$\left(\frac{\beta_2\omega_m L\Delta\omega}{4}\right)^2 = \ln(2) \tag{37}$$

For finding the value of the frequency f_m that yields that condition, it is necessary to express ω_m in terms of f_m, i.e. $\omega_m=2\pi f_m$. But this, in turn, yields an expression that can be reduced by expressing $\Delta\omega$ in terms of $\Delta\lambda$ and β_2 in terms of dispersion D. For $\Delta\omega$ this is done as follows: given $d\omega/d\lambda = -(2\pi c/\lambda^2)$, where c is the speed of light in the free space and λ is the wavelength of the optical signal, it is possible to establish the following correspondence:

$$d\omega = -\frac{2\pi c}{\lambda^2}d\lambda \Leftrightarrow \Delta\omega = -\frac{2\pi c}{\lambda^2}\Delta\lambda \tag{38}$$

Now, for the factor β_2, given that the group velocity, $v_g = L/\tau_g$ where τ_g is the group delay, is related to $\beta(\omega_n)$ as $\tau_g/L = d\beta(\omega_n)/d\omega$, and its derivative is $(d\tau_g/d\omega)/L = d^2\beta(\omega_n)/d\omega^2 = \beta_2$, then $(1/L)(d\tau_g) = d\omega\beta_2$. Thus, the derivative of this expression by $d\lambda$ is $(1/L)(d\tau_g/d\lambda) = (d\omega/d\lambda)\beta_2$. Furthermore, the dispersion, as a function of the wavelength is defined as $D = (1/L)(d\tau_g/d\lambda)$. This means that $\beta_2 = -D(\lambda^2/2\pi c)$. Finally, by substituting $\omega_m = 2\pi f_m$, $\Delta\omega$, in Eq. (38), and the expression for β_2 in Eq. (37), the frequency f_m, which corresponds to the low-pass bandwidth Δf_{lp}, can be expressed as:

$$\Delta f_{lp} = \frac{2\sqrt{\ln(2)}}{\pi D L \Delta\lambda} \tag{39}$$

where the dispersion D has units of ps nm^{-1} km^{-1}, length L is given in km, and the FWHM of the optical source, $\Delta\lambda$, in nm. This means that in the presence of an optical source, like a super luminescent light-emitting diode (LED), the frequency response of the system is low-pass, and its bandwidth is given by Eq. (39). In the context of this chapter, the optical source is an multimode laser diode (MLD). The emission spectrum of this type of optical sources can be modeled by means of an analytical expression as expressed in Eq. (40):

$$P(\omega) = \frac{2P_o}{\Delta\omega\sqrt{\pi}} \exp\left(-\frac{4(\omega-\omega_n)^2}{\Delta\omega^2}\right)\left[\frac{2P_o}{\sigma\omega\sqrt{\pi}} \exp\left(-\frac{4(\omega-\omega_n)^2}{\sigma\omega^2}\right) * \sum_{n=-\infty}^{\infty} \delta(\omega - n\delta\omega)\right] \tag{40}$$

where ω is the angular frequency, ω_n is the central angular frequency, P_o is the maximum power emission, $\Delta\omega$ is the FWHM of the optical source, $\sigma\omega$ is the FWHM of each emission mode and $\delta\omega$ is the free spectral range (FSR) between the emission modes. By using variables Z and W, as defined earlier, and substituting Eq. (40) in Eq. (34), it can be expressed as:

$$F(\omega) = \exp\left(-\left(\frac{\beta_2\omega_m L\Delta\omega}{4}\right)^2\right) * \left[\exp\left(-\left(\frac{\beta_2\omega_m L\sigma\omega}{4}\right)^2\right)\frac{1}{\delta\omega}\sum_{n=-\infty}^{\infty}\delta\left(\frac{\beta_2\omega_m L}{2\pi} - \frac{n}{\delta\omega}\right)\right] \tag{41}$$

The term between crochets indicates the presence of a periodic pattern. The frequency of the first maximum can be determined by equating:

$$\frac{\beta_2\omega_1 L}{2\pi} = \frac{1}{\delta\omega} \tag{42}$$

For finding the value of the frequency f_1 that yields that condition, it is necessary to express $\delta\omega$ in terms of f_1. In a similar way as in Eq. (38), it is possible to establish the following correspondence:

$$d\omega = -\frac{2\pi c}{\lambda^2} d\lambda \Leftrightarrow \delta\omega = -\frac{2\pi c}{\lambda^2}\delta\lambda \tag{43}$$

thus, substituting $\delta\omega$ in Eq. (42), expressing ω_1 in terms of f_1 and using $\beta_2 = -D(\lambda^2/2\pi c)$ then the frequency f_1 can be expressed as:

$$f_1 = \frac{1}{DL\delta\lambda} \tag{44}$$

http://dx.doi.org/10.5772/59081

and, in general, the central frequency of the n -th band-pass lobe is given by

$$f_n = \frac{n}{DL\delta\lambda} \tag{45}$$

where n is a positive integer, dispersion D is given in ps nm^{-1} km^{-1}, length L in km, and the FSR $\delta\lambda$ in nm. The bandwidth of each of these band-pass lobes is equal to:

$$\Delta f_{bp} = \frac{4\sqrt{\ln(2)}}{\pi DL\Delta\lambda} \tag{46}$$

which is twice Eq. (39). The periodic pattern in the frequency response of the system will appear only when an MLD is used in the system. This behavior will allow that microwave signals to be filtered and transmitted over a wide range of frequencies.

8. Experimental setup of optical and wireless transmission

In a first step, the MLD used in this experiment (OKI OL5200N-5) is optically characterized by means of an optical spectrum analyzer (Agilent, model 86143B). Figure 10 corresponds to the measured optical spectrum obtaining $\lambda_o = 1553.53$ nm , $\Delta\lambda = 5.65$ nm , and $\delta\lambda = 1.00$ nm for a driver current of 25 mA. The use of a laser diode temperature-controller (Thorlabs, model LTC100-C) allows us to guarantee the stability of the optical parameters to thermal fluctuations.

In a second step, considering a length L=20.70 km of single-mode-standard-fiber (SM-SF) exhibiting a chromatic fiber-dispersion parameter of D=16.67 ps/nm km. Eq. (45) allows us to determine the value of the central frequency corresponding to the first filtered microwave or first band-pass as

$$f_1 = \frac{1}{DL\delta\lambda} = \frac{1}{(16.67\text{x}10^{-12}\text{seg/nm}\cdot\text{km})\cdot(20.70\text{ km})\cdot(1.0\text{ nm})} = 2.8\text{ GHz}$$

Eq. (39) permits us to determine the value of the low-pass band as

$$\Delta f_{lp} = \frac{2\sqrt{\ln(2)}}{\pi DL\Delta\lambda} = \frac{2\sqrt{\ln 2}}{(\pi)\cdot(16.67\text{x}10^{-12}\text{seg/nm}\cdot\text{km})\cdot(20.70\text{ km})\cdot(5.65\text{ nm})} = 271.85\text{ MHz}$$

Finally, according to Eq. (46), the corresponding bandwidth of the band-pass window is $\Delta f_{bp} = 543.70$ MHz .

At this point, it is well worth highlighting the advantageous use of the chromatic dispersion parameter to obtain the filtered microwave signal. Once the main parameters are known, the topology illustrated in Figure 11 is assembled in order to evaluate the frequency response of the MPF.

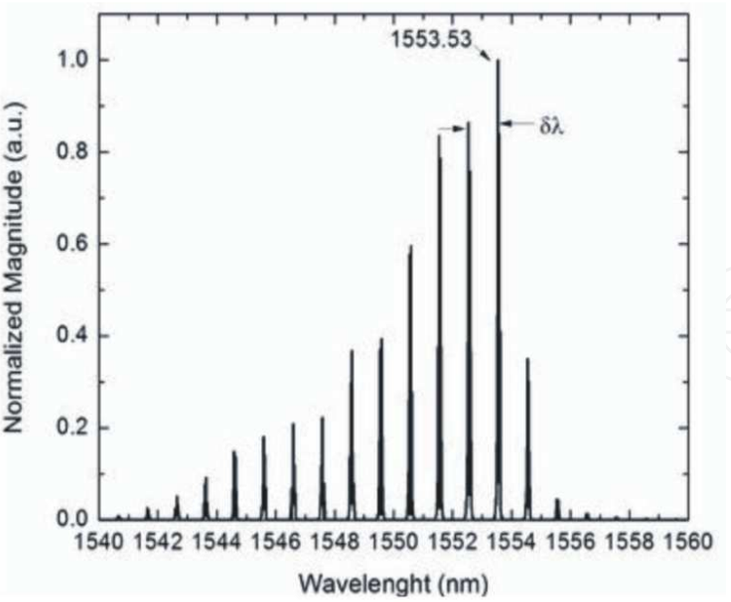

Figure 10. Optical spectrum for the MLD used in the experiment.

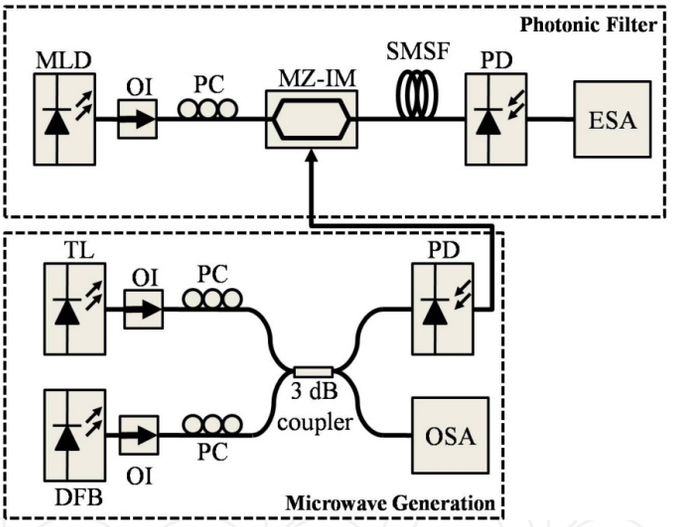

Figure 11. Experimental microwave photonic filter.

At the output of the MLD, an optical isolator (OI) is placed in order to avoid reflections to the optical source. Since the MZ-IM (Photline MX-LN-10) is polarization-sensitive, a polarization controller (PC) is used to maximize the modulator output power. The optical signal is launched into the MZ-IM. The microwave electrical signal (RF) for modulating the optical intensity is supplied by using optical heterodyne as described in Figure 1. The registered frequency response is located from 0.01 to 4 GHz at 0 dBm. The intensity-modulated optical signal is then coupled into a 20.70 km of SM-SF coil. The length of the optical fiber is corroborated by using an optical time domain reflectometer, OTDR (EXFO, model FTB-7300E). At the end of the link, the optical signal is applied to a fast Photo-Detector (PD, Miteq DR-125G-A), and its output connected to an electrical spectrum analyzer (Anritsu, model MS2830A-044), in order to

measure the frequency response of the MPF. Figure 12 corresponds to the measured experimental frequency response where a low-pass band centered at zero frequency and the presence of a band-pass band centered at 2.8 GHz are clearly appreciable.

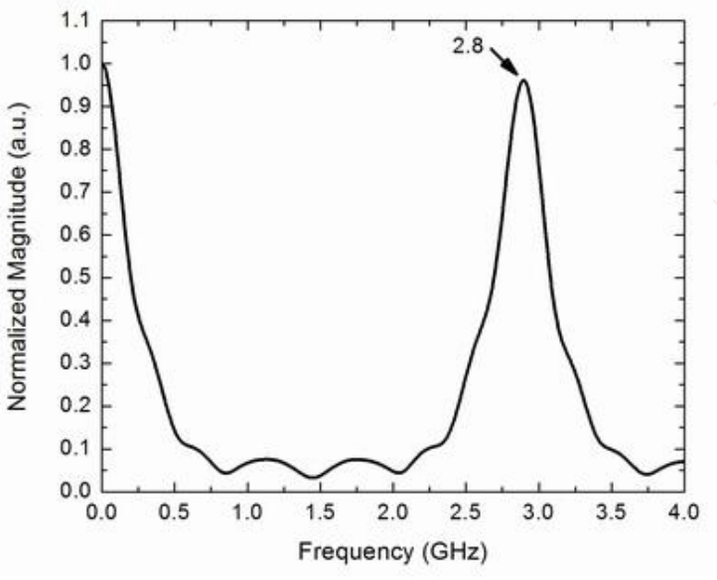

Figure 12. Experimental frequency response of the filter.

The bandwidth of 543.70 MHz associated to the band-pass window centered at 2.8 GHz allows us to guarantee enough bandwidth in case of fluctuations (in the order of nanometers) between mode spacing. On the other hand, a considerable increase on the length of the optical fiber due to thermal expansion is practically impossible. These considerations permit us to guarantee a good stability for the microwave photonic filter. Once the frequency response of the MPF is determined, the setup illustrated in Figure 13 is assembled for carrying out the fiber-radio transmission.

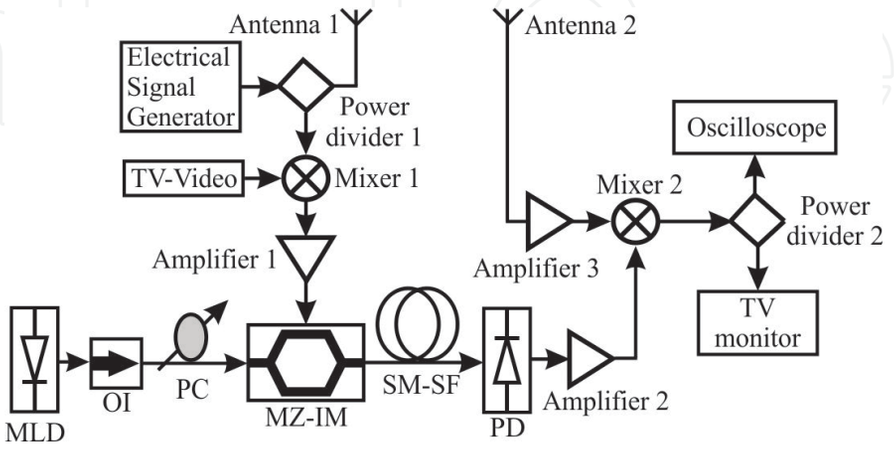

Figure 13. Experimental setup for optical and wireless transmission.

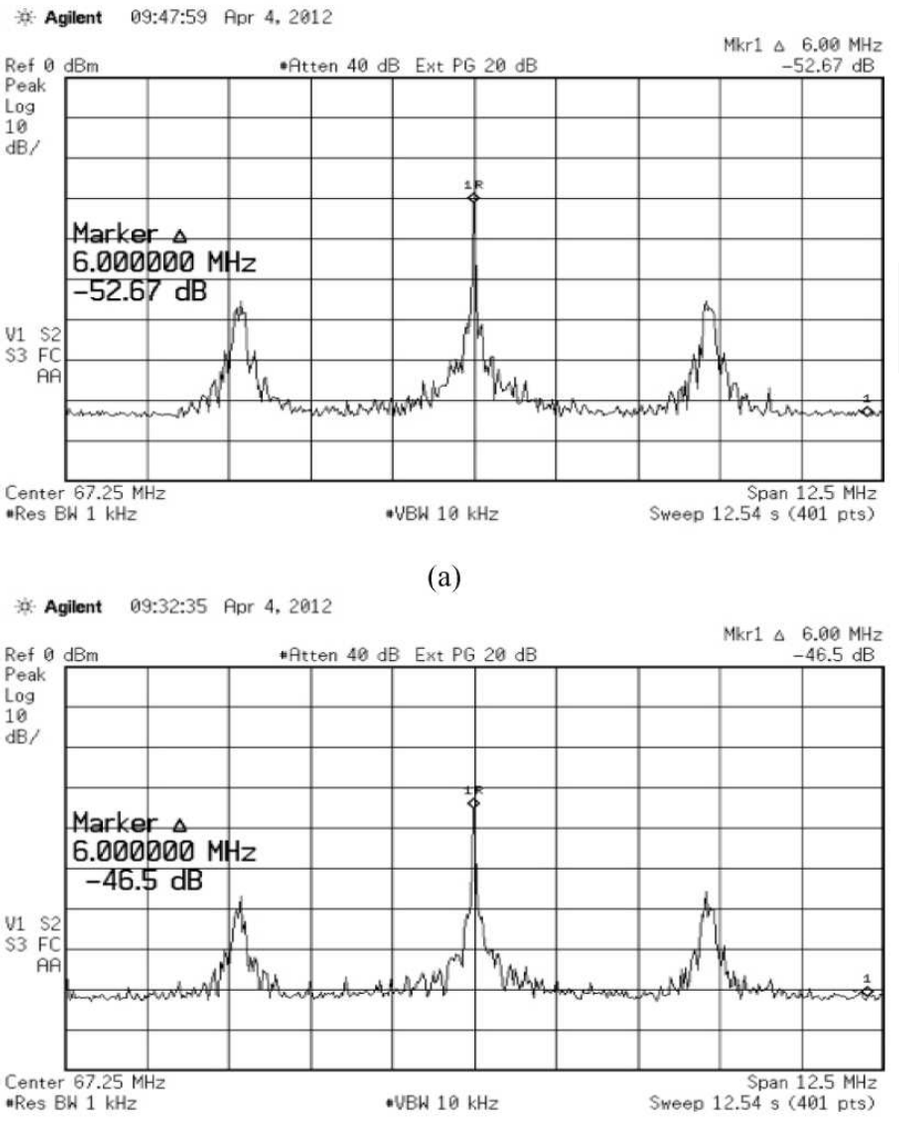

Figure 14. Electrical Spectrums for (a) Transmitted and (b) recovered TV signal.

Now, the electrical signal generator provides a signal of 2.8 GHz at 0 dBm that is used as the electrical carrier and demodulated signal. This signal is separated by using a power divider. Part of this signal is transmitted via radio frequency by the fabricated microstip antenna shown in Figure 5, and the rest is mixed with an analog NTSC TV signal of 67.25 MHz. The resulting mixed electrical signal is then applied to the electrodes of the MZ-IM for modulating the light emitted by the MLD. The modulated light is coupled into the 20.70 km SM-SF coil. At the end of the optical link, the signal is injected to a fast photo-detector (PD), and its electrical output is then amplified and launched to an electrical mixer. Another microstrip patch antenna placed at a distance of 10 meters is connected to a port of the mixer in order to recuperate the microwave signal that plays the role of the demodulated signal. Finally, by using another power divider, recovered analog TV signal can be launched to a digital oscilloscope or to the

http://dx.doi.org/10.5772/59081

electrical spectrum analyzer in order to evaluate the quality of the recovered signal and at the same time display the TV signal on a TV monitor. Figure 14 (a) shows the measured electrical spectrum (Agilent, E4407B) corresponding to the transmitted TV signal where the SNR is 52.67 dB, whereas Figure (b) corresponds to the recovered TV signal with a SNR of 46.5 dB.

Finally, Figure 15 corresponds to a photograph of the screen of the oscilloscope where upper and lower traces are the waveforms of the transmitted and recuperated signal, respectively.

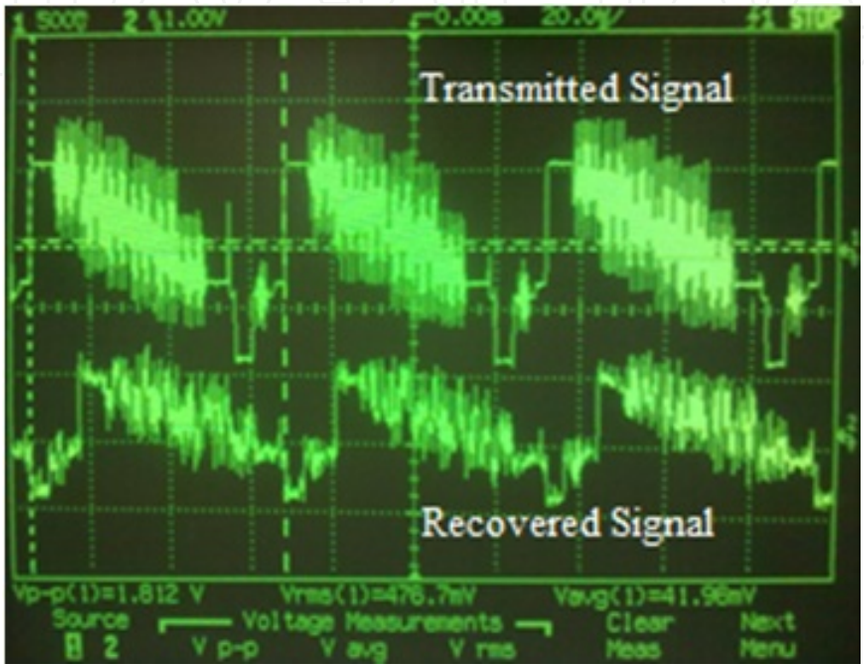

Figure 15. Transmitted and recovered TV signal.

9. Conclusions

Wireless communication systems require compact sources for the generation of mm-wave signals, that must have high spectral purity (linewidth < 100 kHz, phase noise < 100 dBc @100 kHz offset), tuneability, low power consumption and low cost, and although optical heterodyne of two DFB lasers has phase noise of –75 dBc/Hz even at an offset frequency of 100 MHz and it does not very compact, we have demonstrated in this chapter that by using optical heterodyne technique, a TV signal was transmitted and received satisfactory as a result of our proposed communication system generates a microwave carrier and a local oscillator simultaneously ensuring synchronization in frequency as well as in phase between microwave carrier and a local oscillator and avoiding in this case the use of an analog phase locked loop in the receiver to recover the TV information. The authors consider that the first proposed scheme in this chapter is not a truly wireless communication system, since an optical fiber is required to deliver the local oscillator in the receiver, however in order to obtain a wireless communication systems by using optical heterodyne technique, it is necessary to have

collimated beams from optical fiber to photodetectors. On the other hand, due to the fact that the distribution of TV over microwave signals in the electrical domain presents loss associated with electrical distribution lines, the authors consider that the optical fiber is an ideal solution to fulfill this task because of its extremely broad bandwidth and low loss. In that case the distribution of TV over microwave can be directly by using optical fiber. In this way the second proposed experiment in this chapter represents a novel fiber-radio scheme to transmit an analog NTSC TV signal coded on a microwave band-pass located at 2.8 GHz. Filtering of microwave signal was achieved through the appropriate use of the chromatic fiber dispersion parameter, the physical length of the optical fiber, and the free spectral value of the multimode laser. Transmission of a TV signal was achieved over an optical link of 20.70 km, whereas a demodulated signal was transmitted via radiofrequency using the fabricated microstrip patch antennas. Although the distance between antennas was short, this distance can be lengthened if an array of antennas is used. Besides, a mathematical analysis corresponding to the microwave photonic filter was described demonstrating that the frequency response of the microwave photonic filter is proportional to the Fourier transform of the spectrum of the optical source used. The proposed microwave photonic filter represents an interesting technological alternative for transmitting information by using optoelectronic techniques. The results obtained in this work ensure that as an interesting alternative, several modulation schemes can be used for transmitting not only analog information but also digital information. Besides as optical heterodyne technique described here can generate microwaves continually tuned, we can use this feature to transmit several TV signals using frequency division multiplexing schemes FDM [19] and wavelength division multiplexing WDM techniques, not only point to point but also with bidirectional schemes by using simultaneous wired and wireless systems.

Acknowledgements

This work was supported by CONACyT (grants No 102046 and 154691).

Author details

Alejandro García Juárez[1], Ignacio Enrique Zaldívar Huerta[2], Antonio Baylón Fuentes[3], María del Rocío Gómez Colín[4], Luis Arturo García Delgado[1], Ana Lilia Leal Cruz[1] and Alicia Vera Marquina[1]

1 University of Sonora, Department of Physics Research, México

2 National Institute of Astrophysics, Optics and Electronics. Department of Electronics, México

3 Inst. FEMTO-ST, Université de Franche-Comté, Besançon, France

4 University of Sonora, Department of Physics, México

References

[1] A García-Juárez, I E Zaldívar-Huerta, G Aguayo-Rodríguez, J Rodríguez-Asomoza, M R Gómez-Colín, A G Rojas-Hernández. Coherent demodulation of microwave signals by using optical heterodyne technique with applications to point to point indoor wireless communications systems. Journal of Physics:Conference Series 274 (2011) 012008.

[2] Alejandro García Juárez, Ignacio E. Zaldívar Huerta, Antonio Baylón Fuentes, María del Rocío Gómez Colín, Jorge Rodríguez Asomoza, Armando G. Rojas Hernández. Reflected Power Measurement of Antennas between 0 and 4 GHz using Optical Mixing of Distributed Feedback Lasers. Radioengineering, vol. 22, no. 4, December 2013. pp. 1276-1274.

[3] Yang Jing Wen, Hai Feng Liu, Dalma Novak, and Yoh Ogawa. Millimeter-Wave Signal Generation from a Monolithic Semiconductor Laser via Subharmonic Optical Injection. IEEE Photonics Technology letters, vol. 12, no. 8, august 2000, pp. 1058-1060.

[4] Langley L. N., Elkin M. D., Edge C., Wale M. J., Gliese X., Huang X., and Seeds A. J. Packaged Semiconductor Laser Optical Phase-Locked Loop (OPLL) for Photonic Generation. Processing and Transmission of Microwave Signals", IEEE Transactions On Microwave Theory and Techniques, Vol. 47, No. 7, pp. 1257–1264, July. (1999).

[5] J. J. O'Reilly, P. M. Lane, R. Heidemann, and R. Hofstetter. Optical generation of very narrow linewidth millimeter wave signals. Electron. Letters, Vol. 28, No. 25, pp. 2309–2311, (1992).

[6] M. García Larrodé, A. M. J. Koonen, J. J. Vegas Olmos, and E. J. M. Verdurmen. Microwave Signal Generation and Transmission Based on Optical Frequency Multiplication With a Polarization Interferometer. Journal of Lightwave Technology, vol. 25, no. 6, June 2007. pp. 1372-1378.

[7] J. Capmany and D. Novack, "Microwave Photonics combine two worlds," Nature Photonics vol. 1, pp. 319-329, June 2007.

[8] J. Capmany, B. Ortega and D. Pastor, "A Tutorial on Microwave Photonic Filters," Journal of Lightwave Technology vol. 24, no. 1, pp. 201-229, January 2006.

[9] Ignacio E. Zaldivar-Huerta, Alejandro García-Juárez, Pablo Hernández-Nava, and Jorge Rodríguez-Asomoza. Experimental transmission in a fiber-radio system using a microwave photonic filter at 2.8 GHz. IEICE Electronics Express Vol. 10, No. 3, pp. 1-10, February 14 2013, ISSN: 1349-2543.

[10] Thang Tien Pham, Hyun-Seung Kim, Yong-Yuk Won, and Sang-Kook Han. Bidirectional 1.25-Gbps Wired/Wireless Optical Transmission Based on Single Sideband Carriers in Fabry–Pérot Laser Diode by Multimode Injection Locking. Journal of Lightwave Technology, vol. 27, no. 13, July 2009, pp. 2457-2464.

[11] Stavros Iezekiel Microwave Photonics Devices and Applications. John Wiley; 2009.

[12] Kai Chang RF and Microwave Wireless Systems. John Wiley; 2000.

[13] Ramesh Garg, R. B. Garg, P. Bhartia, Prakash Bhartia, Apisak Ittipiboon, and I. J. Bahl, Microstrip Antenna Design Handbook, New York: Artech House Inc; 2000.

[14] J. Liang, C. C. Chiau, X. Chen, and C. G. Parini, "Printed Circular Disc Monopole Antenna for Ultra-Wideband Applications", Electronic. Letter. Vol. 40, No.20, pp. 1246–1247, 2004.

[15] K. L. Wong, T. C. Tseng, and P. L. Teng, "Low-profile Ultra Wideband Antenna for Mobile Phone Applications", Microwave Optical Technolgy Letter, Vol. 43, pp.7-9, 2004.

[16] K. L. Wong, L. C. Chou, and H. T. Chen, "Ultra-wideband Metal-Plate Monopole Antenna For Laptop Application", Microwave Optical Technology Letter, Vol. 43, pp. 384-386, 2004.

[17] Constantine A. Balanis, Antenna Theory-Analysis and Design, Third Edition. John Wiley & Sons, Inc; 2005.

[18] G. Aguayo-Rodríguez, I. E. Zaldívar-Huerta, J. Rodríguez-Asomoza, A. García-Juárez and P. Alonso-Rubio "Modeling and performance analysis of an all-optical photonic microwave filter in the frequency range of 0.01-15 GHz" International Society for Optics and Photonics, 2010. p. 76200B-76200B-12.

[19] Alejandro García-Juárez, Ignacio E. Zaldívar-Huerta, Jorge Rodríguez-Asomoza, María del Rocío Gómez-Colín "Method to transmit analog information by using a long distance photonic link with distributed feedback lasers biased in the low laser threshold current region" Opt. Eng. 51(6), 065006 (2012).